

Bachelor on Aerospace Engineering
2017/2018

Bachelor Thesis
**Experimental Investigation of Non
Linear Flame Dynamics**

Antonio Arcos Rueda

Tutor/es
Yacine Babou
Mario Sánchez Sanz

June 18, 2018



Acknowledgements

First of all, I would like to thank Prof. Yacine Babou for giving me the chance to join this project and at the same time helping me through it. Also I would like to thank Prof. Mario Sánchez for receiving me and making this project become true.

Besides, I would like to appreciate all the support that *Universidad Carlos III de Madrid* has given me in the area of data acquisition and technical facilities.

Finally, I would like to thank Prof. Rafael Molina, director of researching group *Visual Information Processing*, for inspiring and advising me with the image processing algorithms.

Abstract

The main goal of this project is to develop a method to analyze and characterize the evolution of a combustion process by means of image processing. In order to do it some experimental data is required.

Analyzing the flame dynamics by means of the evolution of the instabilities, length and motion ease and improve the characterization of the flame behavior simplifying its further analysis. By implementing elliptical coordinates, "*Block Matching*" and image mapping the process attempts to clarify the motion and development of the combustion in a 2D channel.

All the work was made using the software Matlab, creating a code and implementing several algorithms on it.

Prior to all the study, an experimental procedure was carried out in the laboratories inside Universidad Carlos III de Madrid, in which several mixtures of propane were ignited inside a Hele-Shaw cell and followed by a high speed camera.

Finally, it can be observed how the reaction is more stable and controllable inside the stoichiometric regime, how the curvilinear analysis eases the computations over the instabilities and how the Block Matching algorithm has a perfect implementation into the fluid dynamics field as it becomes so useful to obtain motion.

Resumen

El principal objetivo de este proyecto es el desarrollo de un método de análisis para caracterizar la evolución de un proceso de combustión mediante el procesamiento de imágenes. Para llevarlo a cabo, algunos datos experimentales son necesarios.

Analizando la dinámica de la llama mediante la evolución de sus inestabilidades, longitud y movimiento facilita y mejora la caracterización del comportamiento de la llama simplificando así su análisis posterior. Implementando coordenadas elípticas, "*Block Matching*" y mapeado de imágenes, el proceso intenta esclarecer el movimiento y desarrollo de la combustión en un canal 2D.

Todo el trabajo fue realizado mediante el software Matlab, creando un código e implementando varios algoritmos en él.

Antes de todo este estudio, un experimento fue realizado en los laboratorios de la Universidad Carlos III de Madrid, en el cual varias mezclas de propano con aire fueron encendidas y seguidas por una cámara de alta velocidad dentro de una célula de Hele-Shaw.

Finalmente, se puede observar como la reacción es más estable y controlable sobre el régimen estequiométrico, como el análisis curvilíneo de las inestabilidades favorece su procesamiento y como la herramienta de *Block Matching* tiene una adaptación perfecta al campo de la dinámica de fluidos ya que es muy útil en la obtención de movimiento.

Contents

Acknowledgements	
Abstract	
Resumen	
List of Figures	iv
List of Tables	v
Listings	vi
1 Introduction	1
1.1 Previous Studies	2
1.2 Hele-Shaw Cell	2
1.3 Socio-Economic Impact & Regulatory Framework	3
1.4 Scope of the work	4
2 Methodology	5
2.1 Image Processing	6
2.2 Change of Reference Frame	8
2.3 Data Analysis	11
2.3.1 Peaks	11
2.3.2 Lengths	14
2.3.3 Motion	15
2.3.4 Burnt Velocity	18
3 Results	21
3.1 Peaks	21
3.2 Lengths	23
3.3 Motion	25
3.4 Burnt Velocity	29
4 Conclusion	31
Bibliography	32
Appendices	

A Results $\phi = 0.7$	1
A.1 Image Processing	1
A.2 Peaks & Lengths	2
A.3 Motion	3
A.4 Burnt Velocity	5
B Results $\phi = 0.8$	6
B.1 Image Processing	6
B.2 Peaks & Lengths	8
B.3 Motion	9
B.4 Burnt Velocity	10
C Results $\phi = 0.9$	12
C.1 Image Processing	12
C.2 Peaks & Lengths	13
C.3 Motion	14
C.4 Burnt Velocity	15
D Results $\phi = 1$	16
D.1 Image Processing	16
D.2 Peaks & Lengths	17
D.3 Motion	18
D.4 Burnt Velocity	20
E Results $\phi = 1.1$	21
E.1 Image Processing	21
E.2 Peaks & Lengths	22
E.3 Motion	23
E.4 Burnt Velocity	24
F Results $\phi = 1.2$	25
F.1 Image Processing	25
F.2 Peaks & Lengths	26
F.3 Motion	27
F.4 Burnt Velocity	28
G Results $\phi = 1.3$	29
G.1 Image Processing	29
G.2 Peaks & Lengths	31
G.3 Motion	31
G.4 Burnt Velocity	33
H Results $\phi = 1.4$	34
H.1 Image Processing	34
H.2 Peaks & Lengths	35
H.3 Motion	36
H.4 Burnt Velocity	37

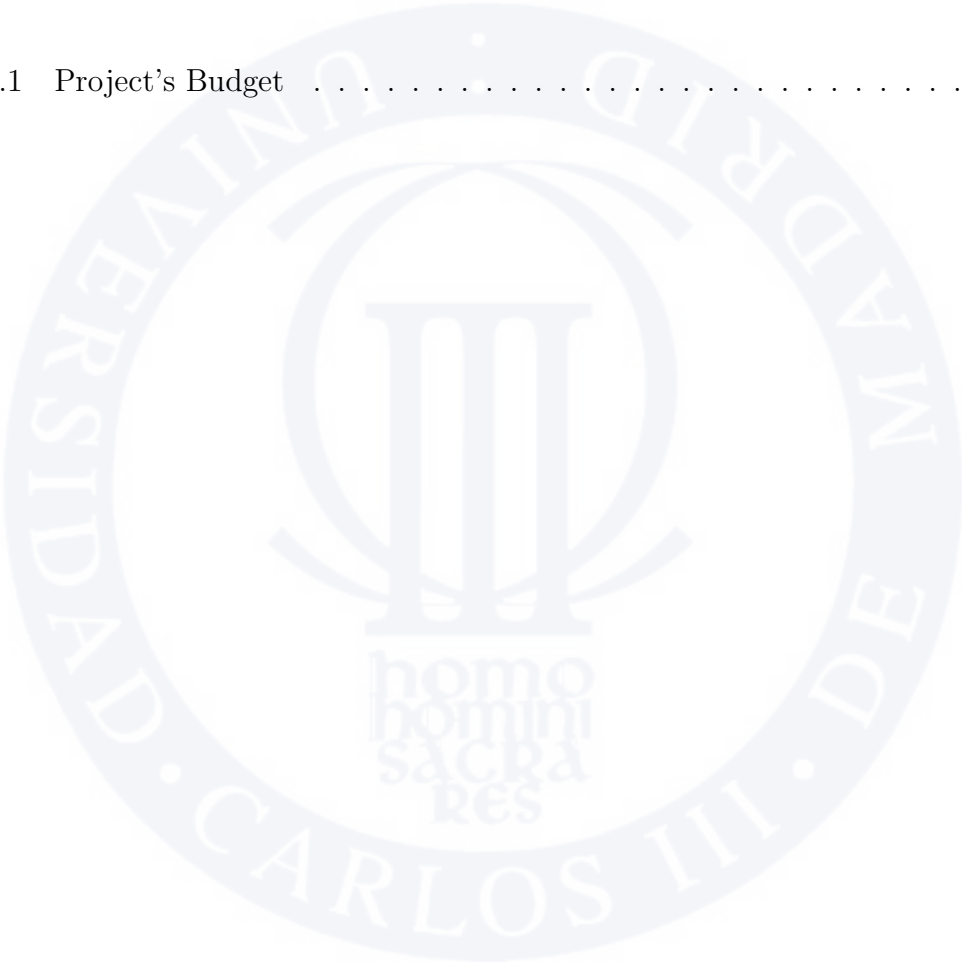
I	Results $\phi = 1.5$	38
I.1	Image Processing	38
I.2	Peaks & Lengths	39
I.3	Motion	40
I.4	Burnt Velocity	41
J	Budget	42
K	Matlab Codes	43
K.1	Core	43
K.2	Peak Finder	54
K.3	Ellipse Fit	61
K.4	XY2SN	71
K.5	Block Matching	74

List of Figures

1.1	Sketch of the Hele-Shaw cell	3
2.1	Flame Evolution with Time	5
2.2	Raw Image	6
2.3	Binarized Image	7
2.4	Outer Contour	7
2.5	Analytic Ellipse [8]	9
2.6	Fitted Ellipse	9
2.7	Inscribing Ellipse	10
2.8	Ellipse Reference Frame	10
2.9	Number of Peaks	11
2.10	Method Error	12
2.11	Smooth Function	13
2.12	Smooth Projection	14
2.13	Flame Length	15
2.14	Lobe Length Evolution	15
2.15	Sectorial Method Error for $dt=0.125$ s and $d\theta = 0.1^\circ$	16
2.16	Block Matching Flow Chart	17
2.17	Motion of the Flame Front	18
2.18	Areas Calculated	19
2.19	Volume of the Flame Evolution	20
2.20	Burn Velocity Evolution	20
3.1	Flame Evolution $\phi = 0.9$	22
3.2	Peaks Evolution with Time	23
3.3	Length Evolution with Time	24
3.4	Lobe Lengths	25
3.5	Radial Expansion	26
3.6	Mid-Combustion Flow Facts	27
3.7	Late-Combustion Flow Facts	28
3.8	Burning Behaviours	29

List of Tables

J.1 Project’s Budget 42



Listings

K.1	Core Code	43
K.2	Peak Finder Code	54
K.3	Ellipse Fitting Code	61
K.4	Ellipse Plotting Code	68
K.5	Projection Code	71
K.6	Bidirectional Search	74
K.7	Motion Estimation	74
K.8	Logarithmic Search	76

Chapter 1

Introduction

Matching between harmonic acoustics and combustion was discovered hundred years ago, since then, a lot of progress have been made in different applications of the combustion search field trying to understand the instabilities generated during the flame propagation. One of the most difficult points for this area is understanding the non-linear flame dynamics that experiments depicts during its analysis. As a non-linear evolution, the flame front of a burned gas would require a deep analysis in its developing in different environments and conditions.

The case of 2D flames experimental analysis could lead to relevant conclusions to several areas of the combustion research where narrow channels appear or simply to small sized combustions, where the disturbances in the flame front are remarkable to the whole combustion process.

The dynamics of a flame contained in the narrow gap between piston and cylinder wall, in a ICE (Internal Combustion Engine) could be studied by this 2D analysis. Also emerging combustion studies are looking forward to small scale engines development in order to reduce the weight, while maintaining the efficiency and power generation of a larger one, so that the two dimensional front flame dynamics could also be applied to model those engines.

Furthermore, the oscillations produced in the combustion chamber by this perturbations on the flame front are a common engineering problem. As it is know all the vibrations produce dangerous pressures and temperatures for the other components of the system as well as mechanical and thermal loading in the framework. All these consequences should be taken into account in the design of the engine generating an increase of emissions and reducing the life-span, operating range and hence efficiency of the engine.

1.1 Previous Studies

First studies of flame acoustics [31] were made in 1878 by J.W. Strutt (Lord Rayleigh) where he explained the consequences of the vibration of air masses in reciprocating engines relating them with the Newton's velocity of sound postulation and Laplace's theory of the propagation of sound.

Later on, more studies about instabilities in engines and combustion oscillations emerged [14] trying to explain the behavior of the flames and how their instabilities were produced [26]. However, it was in 1938 where the first study [16] of quasi-2D configuration flame fronts were made by Darrieus and later by Landau (1944) [25]. Their analysis concludes with an analytical expression to explain the thermal expansion and buoyant instabilities considering both fluids constant in properties with an infinity small perturbation in the flame front.

Years later, in 1958 the effects of viscosity in the flow were included by Saffman [34] ; leaving only the effects of the thermal diffusion to be added. Finally it was in the XXI century when S. H. Kang [23] include those instabilities by applying the Navier-Stokes formulation, revealing the effects of heat and momentum losses on the flame front stability.

In resume, up to now, four type of instabilities should be considered during the analysis of the front flame dynamics:

- The Rayleigh-Taylor (RT) instability: due to buoyant convection
- The Darrieus-Landau (DL) instability: due to density across the front
- The Saffman-Taylor (ST) instability: due to viscosity changes
- The diffusive-thermal (DT) instability: due to the difference between the molecular and thermal diffusion coefficients

1.2 Hele-Shaw Cell

During this paper, a particular experiential configuration would be explained: the Hele-Shaw cell [18]. This experiment consists on the study of the non-linear, two-dimensional evolution of the flame front of two immiscible fluids between two parallel, polymer-made, rectangular plates. The evolution of the flame is recorded by a high-speed camera from the spark ignition to the end of the propagation bounds.

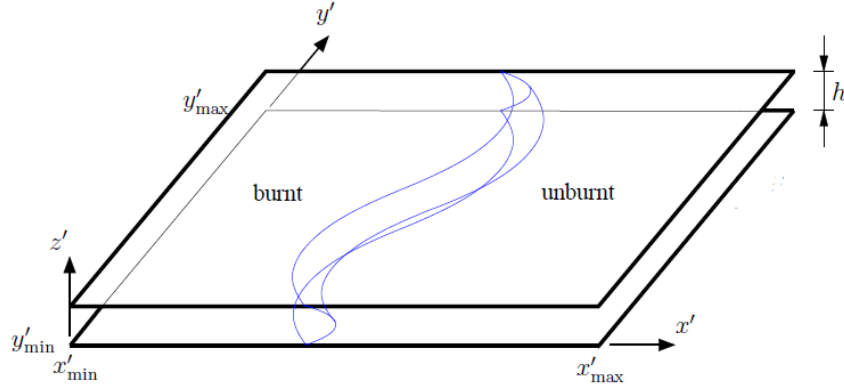


Figure 1.1: Sketch of the Hele-Shaw cell

In this experiment the space between the plates (h) is negligible (10 mm) compared to the x and y coordinates (1 m and 0.5 m) for the system and so on the problem is analyzed for 2D. During this experiment an open-open configuration and propane gas is used for the combustion process; analyzing several equivalence ratios of the mixture air-fuel, from lean to rich combustions.

During its cell propagation the flame front would develop several instabilities due to the presence of viscosity variations, thermal-diffusion, buoyant convection and density changes. Each one of these parameters contributes to the destabilization of the flow, modifying the flame dynamics and leading to a non-linear regime.

The experiment is run by a glow plug, that when electrified, by Joule effect the tip ignites the unburnt gas after injecting it inside the cell; starting the flame.

1.3 Socio-Economic Impact & Regulatory Framework

Engines and combustion process surround us nowadays and a full understanding of them would lead to release the constraints related with them optimizing innumerable processes and designs. Moreover, describing the behaviour of fluids, interphases and instabilities has implementation on the major researching areas, having a positive economic, environmental and industrial potential.

The first and major idea of this study is focused on internal combustion and then improving engines combustion efficiency. Nowadays, the emissions of total hydrocarbon (THC), non-methane hydrocarbons (NMHC), nitrogen oxides (NO_x), carbon monoxides (CO), particulate matter (PM) and carbon dioxide (CO_2) is strictly regulated and revised by the European Commission [13] for most of the vehicle types: road, rail, air and maritime transport; representing around a quarter of Europe's

gas emissions .

Accordingly to Cleansky2 projects [1] development of the engine industry as well as a "*green*" aerodynamics design could contribute up to a reduction of 32% of CO_2 emissions and 40% of NO_x emission. Nevertheless these combustion improvements not only apply to emissions but noise, having a good economic impact during design, production and fuel saving. If instabilities during combustion could be predicted, better rotordynamics designs could be implemented reducing noise up to 15.7 dB and noise area up to 86% in regional missions.

Concerning the regulatory framework of the project itself, it can be seen how there are not any specific rules applying to it, as the whole analysis was computer-based while the experimental part of it was carried out by the university under the pertinent safety measures.

1.4 Scope of the work

During this project the importance of understanding combustion and in particular nonlinear flame dynamics is acknowledged. Exploring and analysing techniques to simplify and reduce the research complexity using image algorithm, mapping or regression are just some methods used during the following sections.

The core of the document is based on four chapters, which are briefly commented below:

- Methodology: it is constituted by three parts. In each one of them one process of the analytic and theoretical bases of the process is explained: how the results are obtained from the raw images to the final data, passing through the image processing, the change of reference frame or particular data obtaining.
- Results: divided in four separated data, in each of them the final results are commented and contrasted with the theoretical analysis of previous studies, including the influence on combustion and fluid dynamics of the equivalence ratio or time.
- Conclusions: during this section a complete summary of the whole project is done in order to give a broad perspective of the study.
- Appendices: some of the results obtained during the analysis are attached to deeper information as well as some additional information.

Chapter 2

Methodology

The Hele-Shaw cell analysis consisted on processing the high-speed camera pictures of the flame develop in order to obtain the evolution of the instabilities, the length of the flame and the flame front speed along the time, to once having them characterize the combustion.

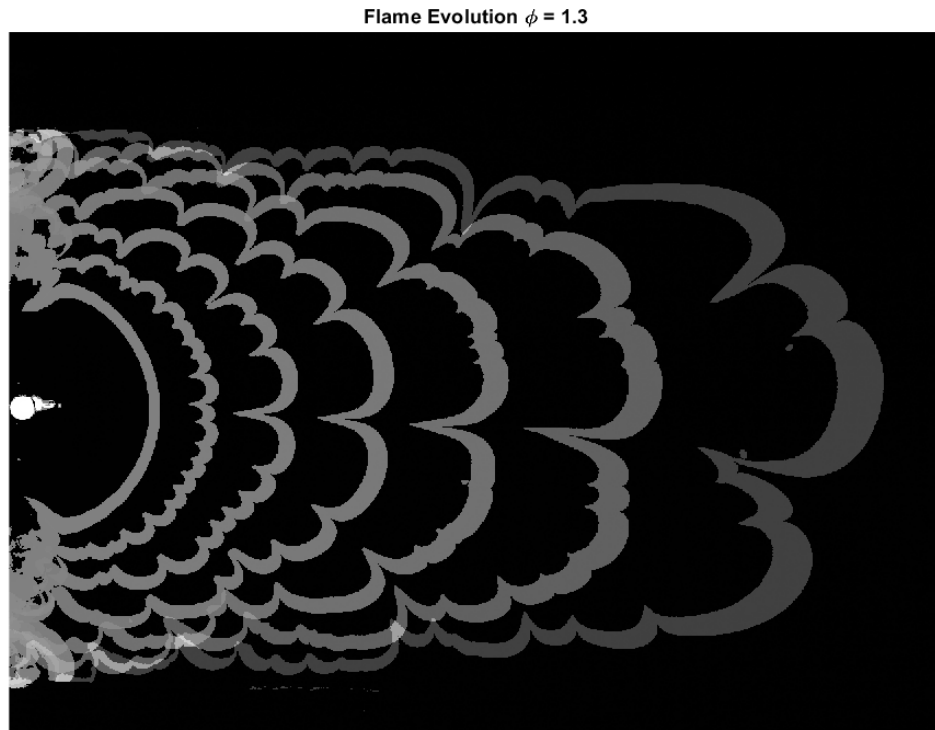


Figure 2.1: Flame Evolution with Time

In order to do so, a Matlab software was implemented to get the information from the pictures, process it in order to be meaningful, extract the required data from it and finally get the useful information for the analysis.

2.1 Image Processing

The first step in the whole analysis is to extract the useful information from the images taken during the experiment.

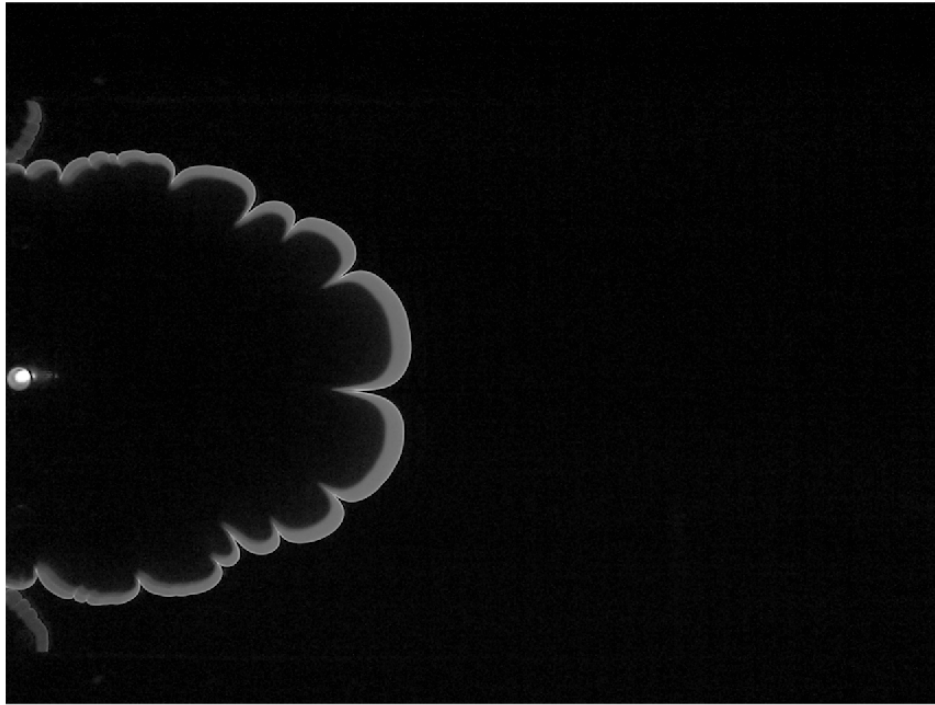


Figure 2.2: Raw Image

To achieve an accurate analysis of the front flame, each frame of each configuration should be fitted to the experiment reference system: the rectangular plates; so some parts of the images must be removed, as the picture of them reveal more than the plates frame. Also the first part of the x axis is removed in order to achieve a cleaner analysis of the front, avoiding some interferences with the plug while processing them.

Once the images are perfectly fitted into the required reference system, the flame front could be extracted from the image by binarizing it and extracting the contours of the frame, an adaptive thresholding was used in order to achieve the cleanest information in each frame, due to the light evolution with the combustion of the propane.

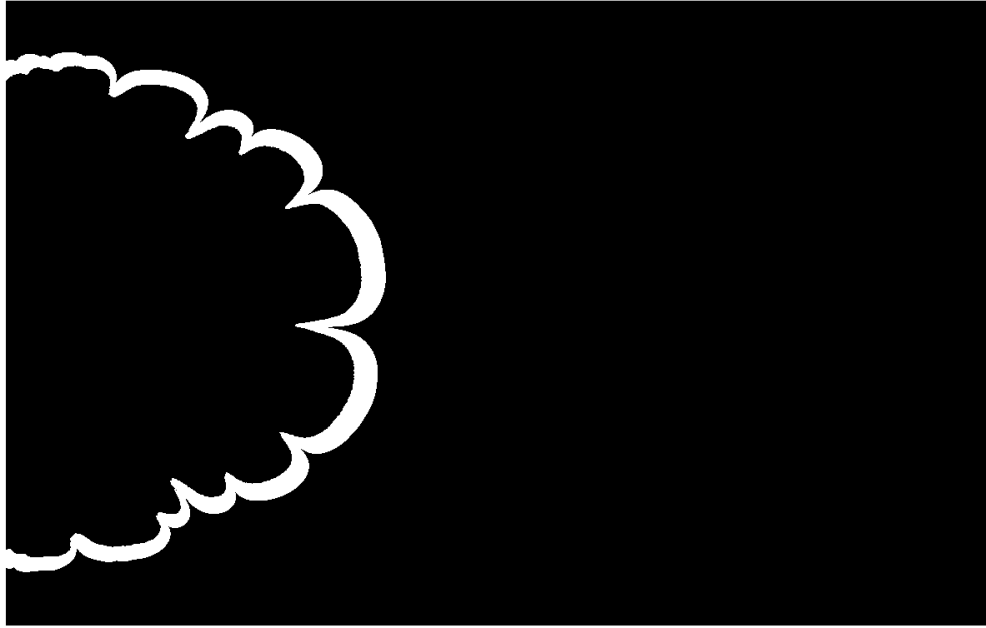


Figure 2.3: Binarized Image

Once the B&W images are obtained and are contours selected, the inner flame contour must be erased from the analysis as the relevant information is obtained from the outer one due to its regime of interphase between the burnt and unburned gases.

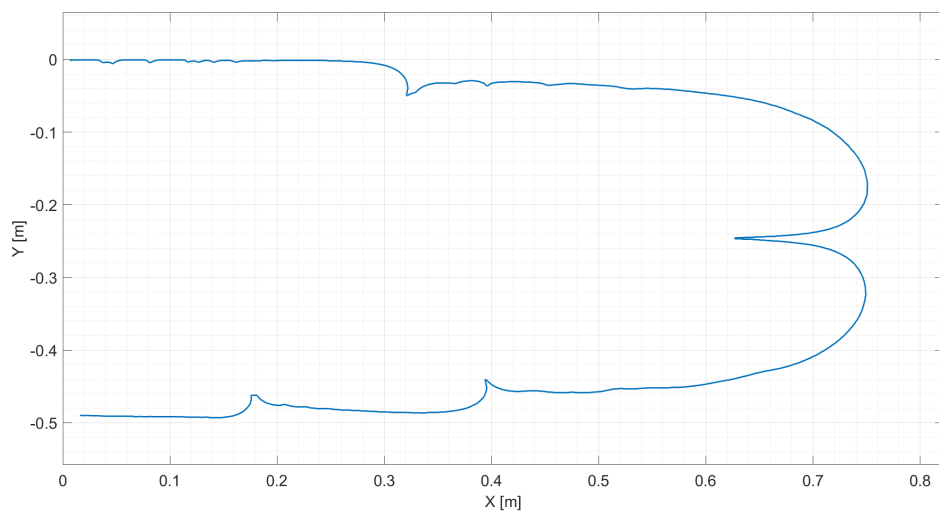


Figure 2.4: Outer Contour

2.2 Change of Reference Frame

The analysis of the evolution of the flame dynamics could be so complex if it is analysed through the X-Y axis of the experimental frame. However, the evolution of the flame length, the instabilities, etc of the flame could be easily extracted with an adapted reference frame fitted into the flame front.

As it was shown in previous papers [8], the conic curve which enables the easiest analysis for the front of a Hele-Shaw cell propagating flame is the ellipse, as it can properly fit the circular shapes of the beginning as well as the conic shapes of the end.

From the previous steps, the outer flame front was cleanly extracted from the images, so the ellipse could be fitted into it. Three different methods were proposed to do that:

1. To create analytically an ellipse, in which the minor axis is the mean between the maximum and minimum Y values of the front; and the mayor axis is the maximum X value of the front [8].
2. To numerically fit an ellipse into the flame front points using a Matlab approximation program ("*fitellipse*") [6] (Appendix K.3).
3. Mapping the contour of the flame in each flame and analytically creating an ellipse in which the minor and mayor axes are selected to exactly inscribe the flame front.

The differences between the three different methods are shown in the following images:

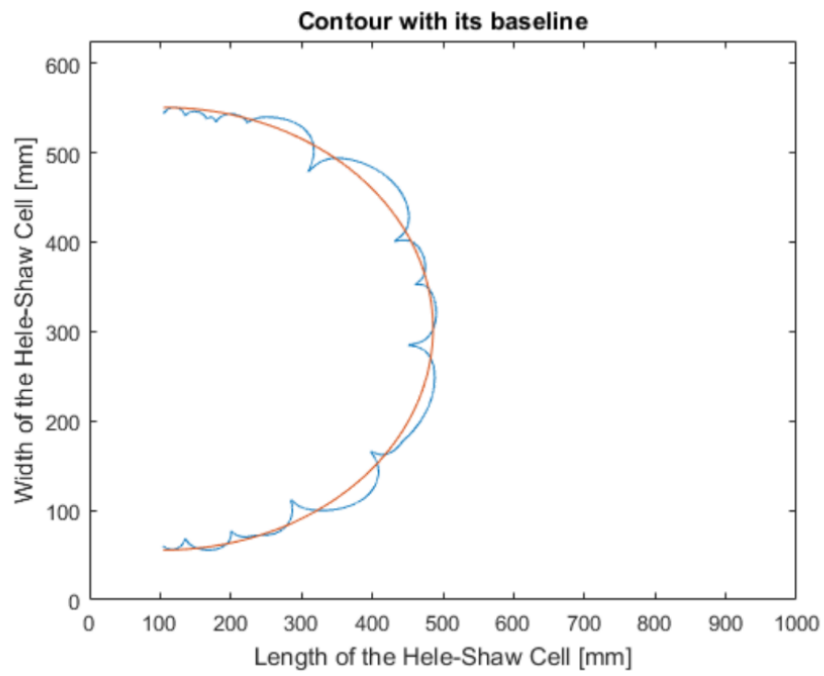


Figure 2.5: Analytic Ellipse [8]

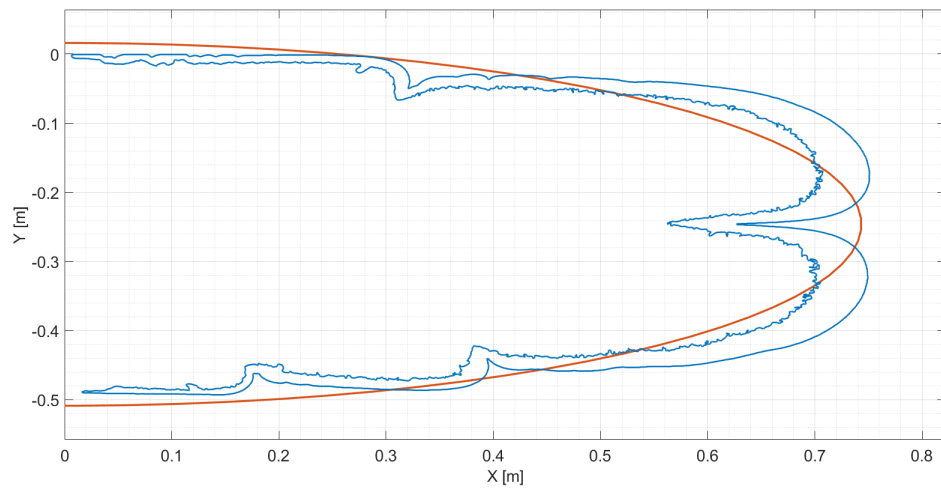


Figure 2.6: Fitted Ellipse

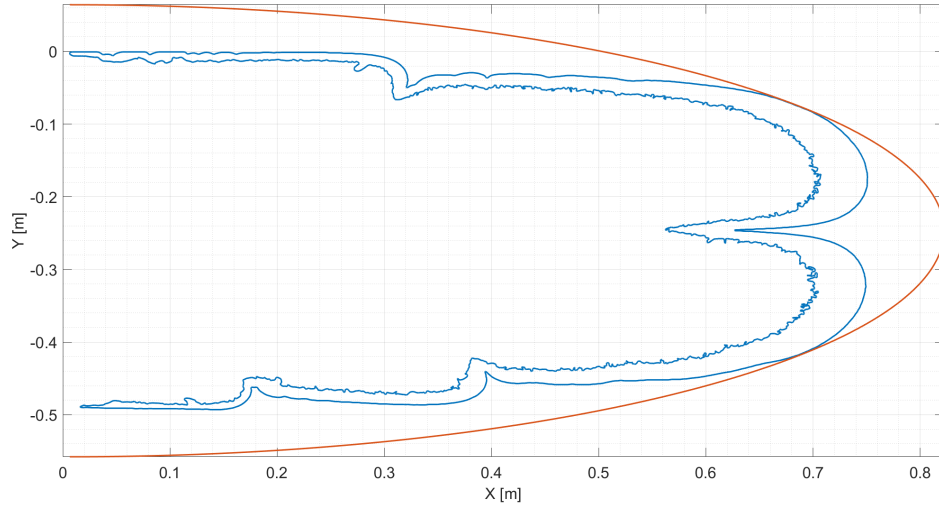


Figure 2.7: Inscribing Ellipse

As it could be seen the analytical method offers a good fit for the first instants of the flame, when the instabilities generate small and similar lobes, but it loses accuracy when the flame develops. The second method, however, offers a better fit for the late parts of the evolution as well as in the beginning of the flame. However due to post analysis in section 2.3.1 of the flame the third method is used, which returns better results for the signal mode of the contour.

The selection of the ellipse for each frame is a key factor as it would be the baseline of the analysis reference frame. This change of reference frame is modelled by the Matlab function `"xy2sn"` [35] (Appendix K.4) which transforms Cartesian coordinates to channel fitted coordinates as shown below:

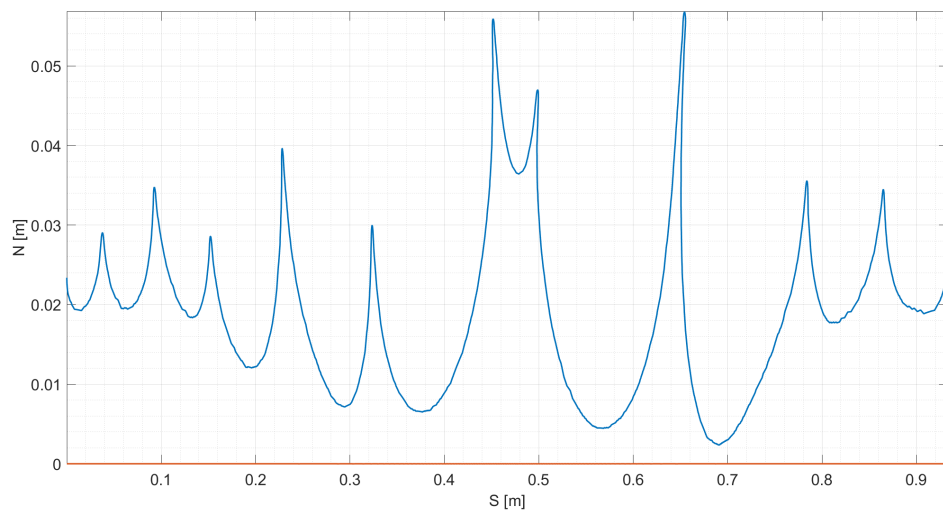


Figure 2.8: Ellipse Reference Frame

In Fig.2.7 and Fig.2.8 it can be appreciated how the flame front (blue) goes from cartesian coordinates to the ellipse (red) coordinates.

Once the flame front is expressed in this coordinate system, it is completely ready for the further analysis.

2.3 Data Analysis

The flame dynamics could be analyzed in different parameters [32] [29], but in this study, the procedure would be focused on the flame front length, the volume burnt and the number of peaks of the front. With those values the evolution of the instabilities could be characterized and later on the front dynamics [12] [21]. All the images and data provided in the following section belongs to the $\phi = 1.3$ experiment and $t=0.15s$.

2.3.1 Peaks

First, the number of peaks of the front is extracted finding the maximums in the fitted coordinates [38] (Appendix K.2). To do that a threshold of a pixel size was chosen to avoid perturbations and noise of sub-pixel amplitudes.

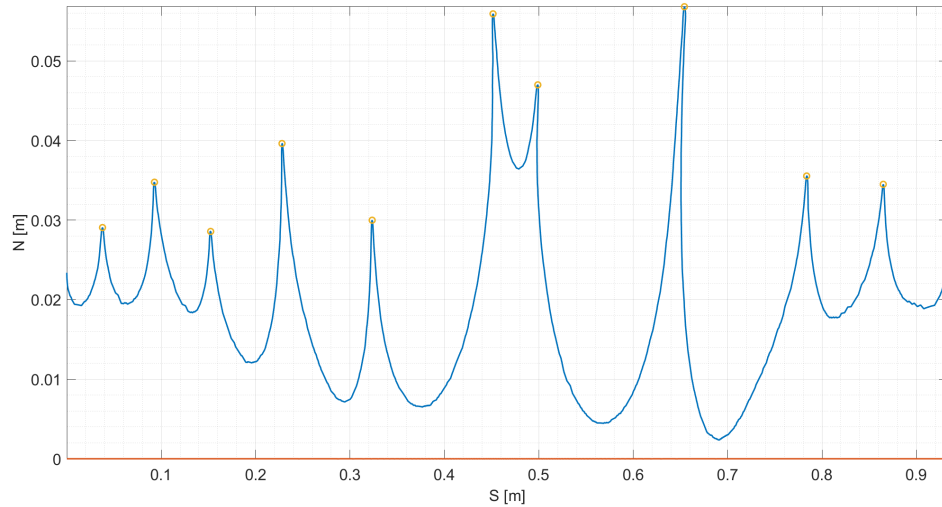


Figure 2.9: Number of Peaks

However, this method causes the appearance of non-existing peaks for the flame front, particularly in the early stages of the evolution. This problem can be observed in Fig. 2.10.

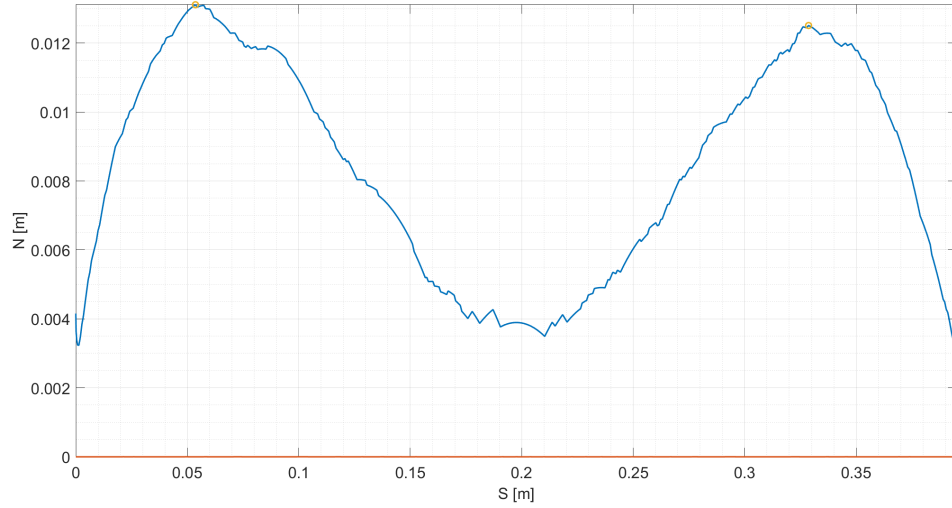


Figure 2.10: Method Error

In order to avoid this error, a second reference frame is selected and again processed through *"xy2sn"*. In this case, the projecting reference frame would be a smoothed function of the previous elliptical data.

Here comes one of the most critical parameters for the analysis of the next sections: defining a good smoothing method as well as the span fitted to each one of the frames. For the method, Matlab offers several tools, the most remarkable ones are: *'moving'*, *'lowess'*, *'loess'*, *'rloess'* and *'rloess'*. Each one of them correspond to a local least square regression, as this case could be related to compound harmonic, the *'rloess'* is the best method.

In order to fix a span for the smoothing process, an analysis of the evolution of the length of the contour with time and the evolution of the number of peaks with time was made. The first parameters evolve parabolic while the peaks' evolution look like a third degree polynomial. In both cases, the coefficients vary with the equivalence ratio.

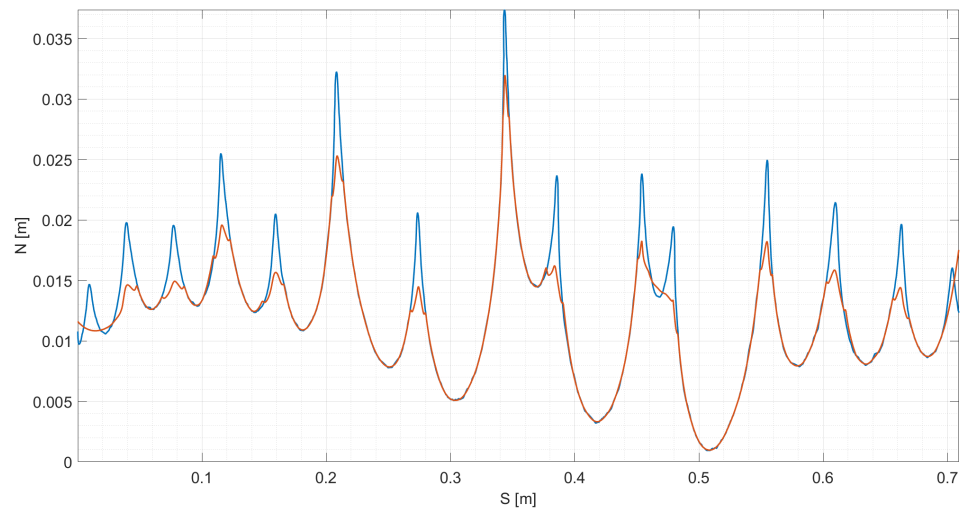
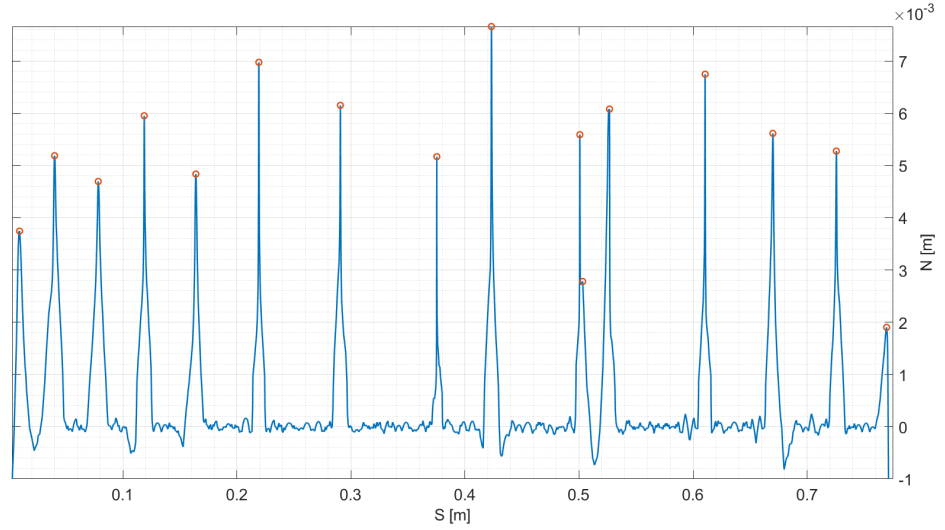
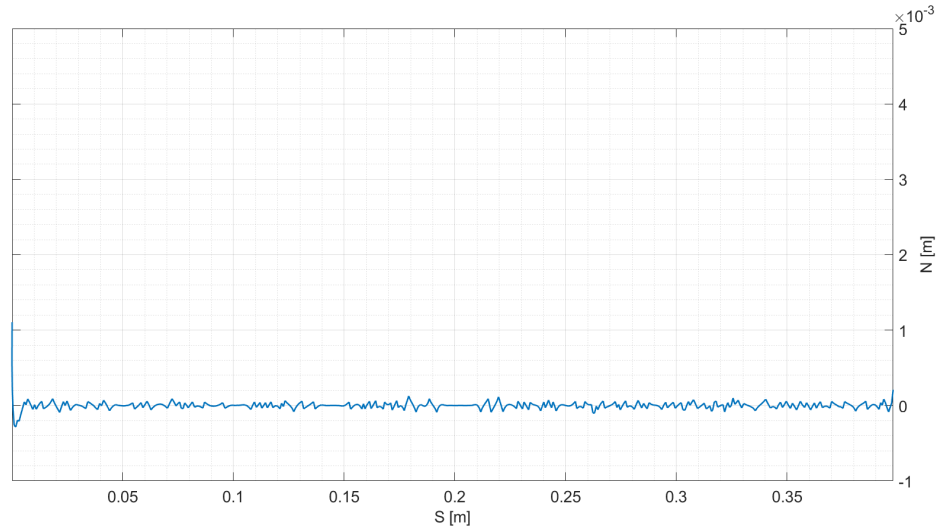


Figure 2.11: Smooth Function

Once these parameters are set, the smoothing and projection is applied and the number of peaks is corrected as Fig.2.12 depicts.



(a) Mid Combustion



(b) Early Combustion

Figure 2.12: Smooth Projection

2.3.2 Lengths

Lately, the total flame length and the lobe length are calculated by the arc length integral for the whole flame and between peaks:

$$L_f = \int \sqrt{1 + \left(\frac{dy}{dx}\right)^2} dy \quad (2.1)$$

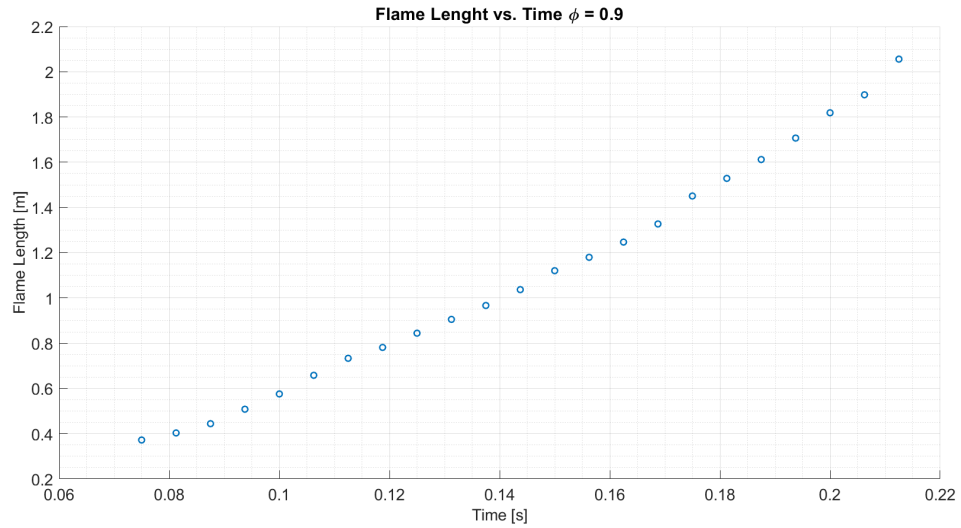


Figure 2.13: Flame Length

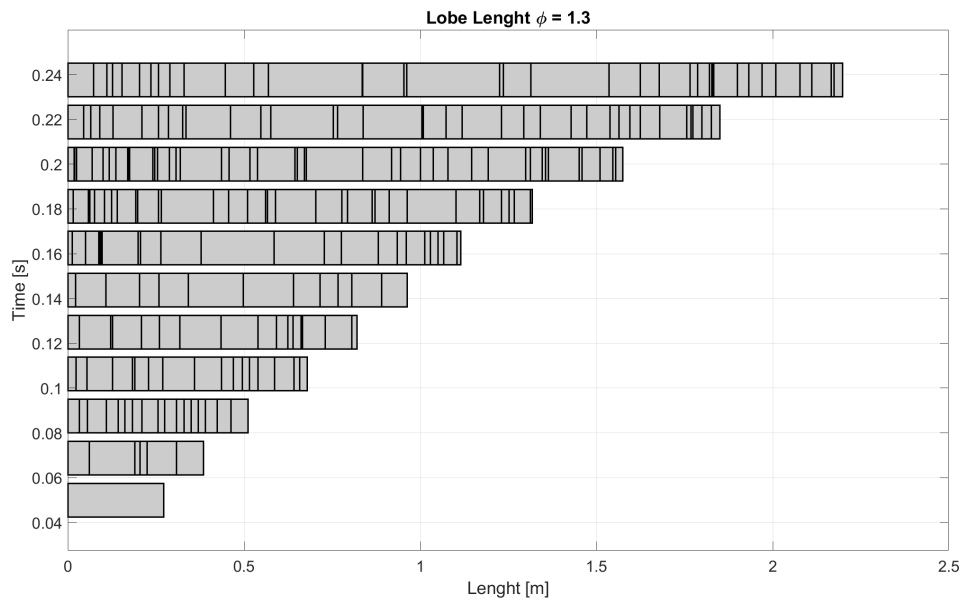


Figure 2.14: Lobe Length Evolution

In Fig. 2.13 it can be observed how the flame length increases through time while in Fig. 2.14 the length of each lobe in the flame increases or decreases randomly, keeping the same behaviour for the total length.

2.3.3 Motion

Once obtained the evolution of the length and number of instabilities with time, it is time to compute the velocity of the flame itself. In this purpose several methods

were investigated.

In the first one a sectoral method was applied in which each one of the parts of the flame landing in this θ value predefined corresponds adimensionally to the same θ parts of the previous frame. This method applies good and reasonable results to values of θ and frame step as small as possible returning feasible velocities with $d\theta$ and dt . However, as these values are increased in order to have a reasonable computing time, it could be appreciated a huge error in the estimated motion direction.

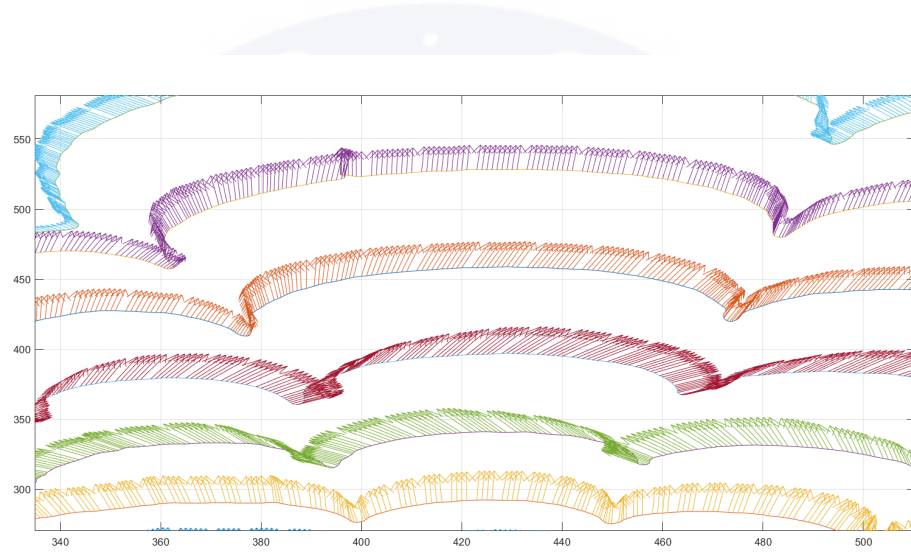


Figure 2.15: Sectorial Method Error for $dt=0.125$ s and $d\theta = 0.1^\circ$

In other hand, several analytical methods based on differential equations were proposed in order to characterize the propagation and perturbations[4] [24] [5] on one FDF (Flame Describing Function). In some other studies [7] the velocity of the 2D flame front is derived considering that the motion is fully determined by the DL instability, i.e. non-viscous flow, no thermal-diffusion instability or external turbulences; which nearly apply to the situation studied.

Although those studies could analytically describe the motion of the flame with a good accuracy they could not be implemented into the code program as several of the conditions or constants were not fulfilled nor measured by the experiment done in the Hele-Shaw Cell.

Finally, once the analytical method based on fluid dynamics and the mathematical path based on sectors were studied, the last chance was to analyse the problem with image treating. This area of study is based on a set of techniques applied to digital images in order to obtain some data on them [37] [19]. In the case studied, as the velocity of the flame is required, the *Block Matching* algorithm will be implemented [30].

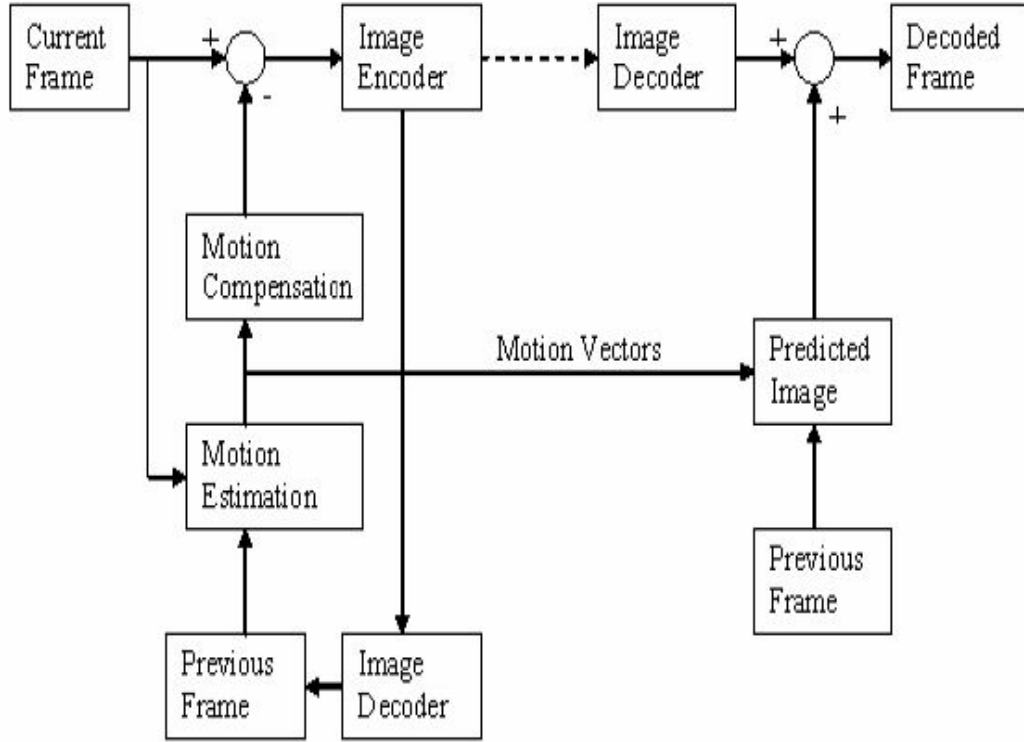


Figure 2.16: Block Matching Flow Chart

Block Matching techniques are not a new development, since their creation they have been widely used for video or image processing in several research fields as medicine [28] [20] in order to track some particularities through medical imaging; video coding [9] [15] with application to resolution improvement, traffic control [36], meteorology [17] or face detection [27]. However, this is one of its first applications into the engineering area and more precisely the first one in the fluid dynamics study, which makes this application an interesting algorithm for local velocity or motion approaches in the complexity of non-linear dynamics.

This algorithm [10] is a video processing sub-pixel motion estimation method for motion deblurring. The basis of the algorithm is to divide each frame of the film into several blocks of n pixels and assign them several properties depending on the grey scale, the position, the motion, etc and compare each one of them with each one of the blocks of the previous frame in order to find the most similar one and corresponding them. Once both blocks are matched, the motion vector and the velocity are easily obtained.

Inside this method several paths to take in the searching of the matching blocks and so several sub-methods exist. For the case studied due to the simplicity and size of the frames, the *Two Dimensional Logarithmic Search* was implemented [22], this method was proposed by J. Jain and A. Jain to be more accurate especially when the frames are large. Also a frame step of $t = 0.125$ s and a filter of order three

($> 10^{-3}$) was selected to improve the results returned by the algorithm.

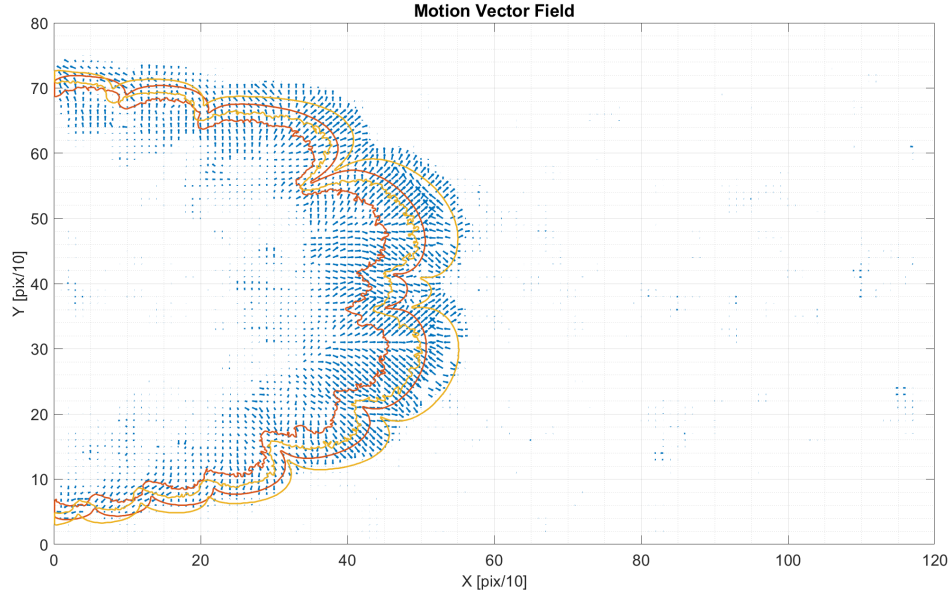


Figure 2.17: Motion of the Flame Front

As it could be seen in Fig.2.17 the method not only takes the motion of the n frame front with respect to the $n+1$ one, but also the near the burnt and unburned gases, which is pretty interesting in order to estimate the evolution of the instabilities of the flame.

2.3.4 Burnt Velocity

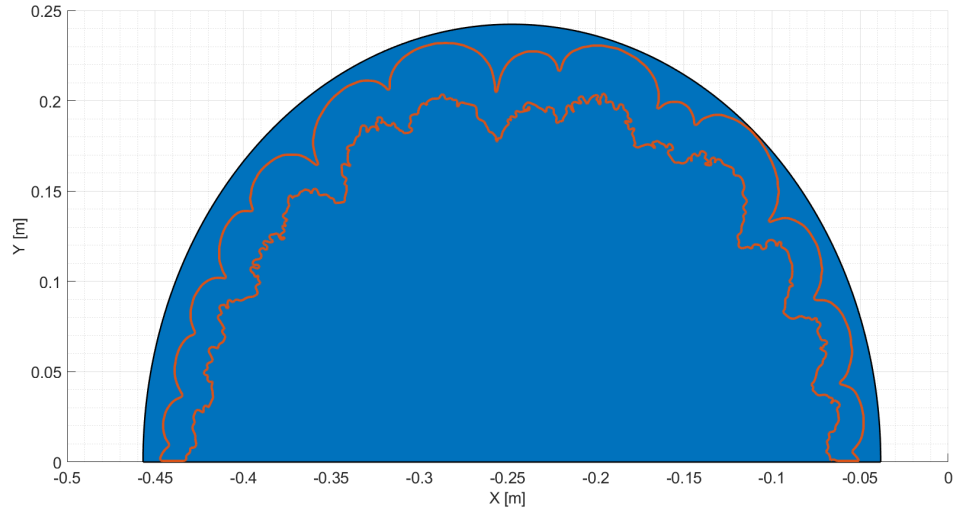
Once the local velocity field is computed, in order to estimate the global advance of the front flame, it would be useful to analyse the burning velocity. In this case, it would be implemented proportional to the volume of the flame.

As it was showed before, the flame evolves with time creating an expanding contour and so a volume for the flame can be estimated. This volume will be assume to maintain its thickness constant during the whole process due to the 2D approximation of the Hele-Shaw cell, however, its horizontal section will change with time increasing its value. In the other hand, in order to adimensionalise the results, a new variable would be defined, X which can be expressed as the formula below:

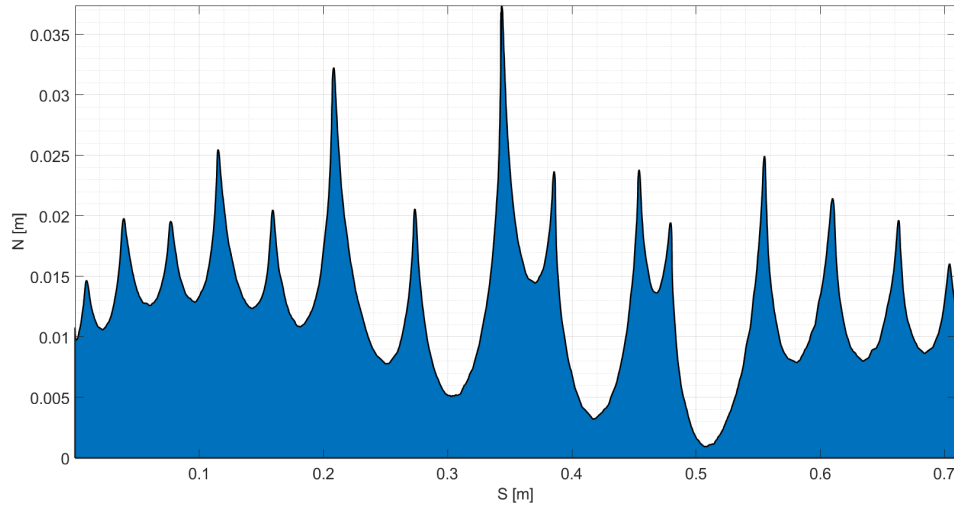
$$X = \frac{V_{burnt}}{V_{total}} = \frac{h \int y dx}{V_{total}} \quad (2.2)$$

Where, V_{total} is the whole cell volume ($0.5 \times 1 \times 0.01$ m), and x and y are the contour coordinates of the front flame.

Due to the complex geometry generated by the instabilities in the last stage of the combustion, the numerical integration of the contour returns a wrong area. In order to avoid that, the area would be analysed as the difference between the inscribing ellipse area Fig. 2.16 (a) and the contour projection over the ellipse area Fig. 2.16 (b). The method is illustrated in the following figure:



(a) Ellipse Area $\phi = 0.9$



(b) Contour Projection Area $\phi = 0.9$

Figure 2.18: Areas Calculated

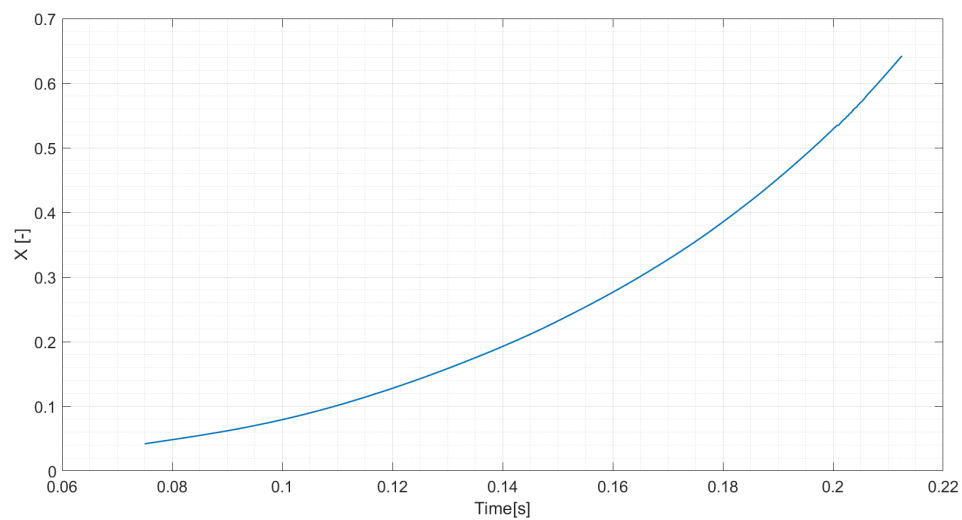


Figure 2.19: Volume of the Flame Evolution

At this time the volume evolution of the flame is obtained and a good approach of the burnt velocity would be its derivative. So another variable will be analysed with respect to time: $\dot{X} = \frac{dX}{dt}$. The graph below show the results for this velocity:

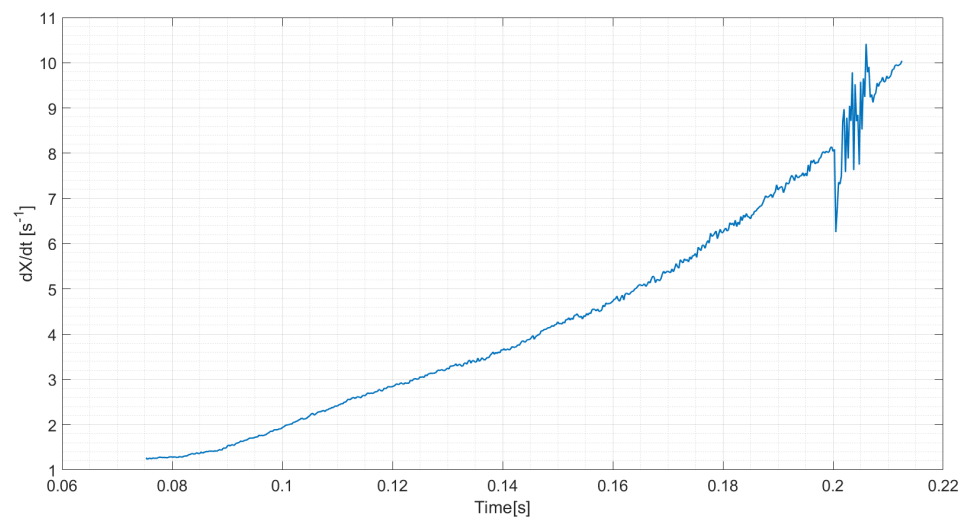


Figure 2.20: Burn Velocity Evolution

Chapter 3

Results

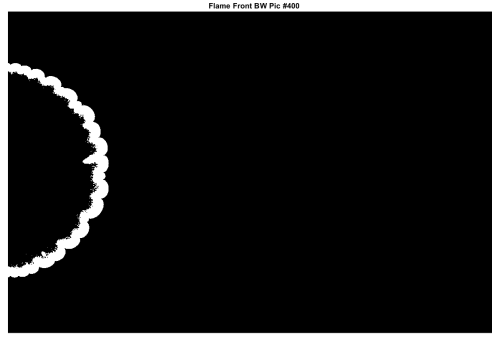
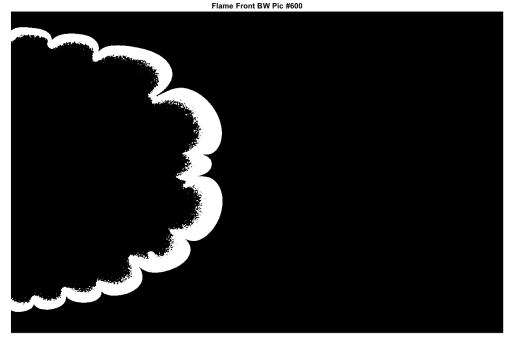
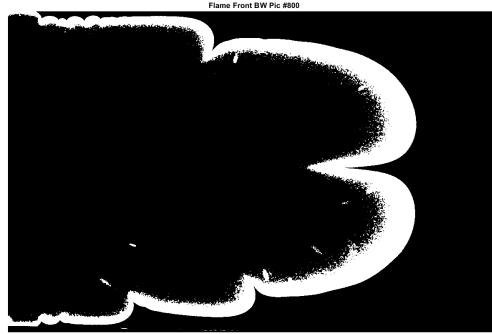
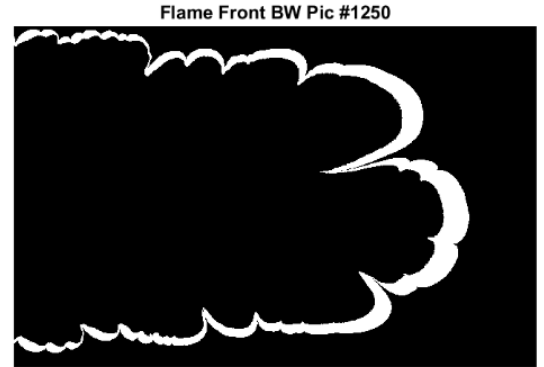
The previous process was applied for different equivalent ratios (ϕ) of the mixture from $\phi = 0.7$ to $\phi = 1.5$. to see how this parameter affects to the flame dynamics.

Results for different equivalence ratios are fully detailed in the attached appendices A-I. In results refereed to $\phi = 0.7$ and $\phi = 1.5$ it will be observed some characteristics that differ from the other results, these errors are due to the image high speed camera shutter opening, that in order to capture at the same frame rate it does not open as much as needed in order to ensure a good lighting and so the images captured are too dark for a high resolution binarizing process.

3.1 Peaks

Looking carefully to the results for the evolution of the peak's evolution it could be easily seen how they have for all the equivalence ratios three stages [2]:

1. The flame front starts to instabilizate just after the ignition and the number of instabilities grow linearly Fig. 3.1 (a).
2. The instabilities start to grow in size and amplitude merging between them as they become bigger and bigger Fig. 3.1 (b).
3. Reaching the limits of the cell some small instabilities appear at the edges of the flame Fig. 3.1 (c). Also some instabilities arise at the central lobes due to the flame stretching only for rich configurations Fig. 3.1 (d).

(a) Evolution $t=0.1$ s Stage 1(b) Evolution $t=0.15$ s Stage 2(c) Evolution $t=0.2$ s Stage 3(d) Evolution $t=0.3125$ s Stage 3 $\phi = 1.4$ Figure 3.1: Flame Evolution $\phi = 0.9$

From these parameters it also could be seen how the lean mixtures are much more stable in the combustion than the rich ones, as they produce less number of instabilities with the pass of the time and also in the third stage of the evolution no instabilities are created in the central part.

This behavior is produced by the difference in density, viscosity and diffusion coefficient of the propane, which as is added to the mixture increases these properties and so the difference with respect to the unburned gas [33].

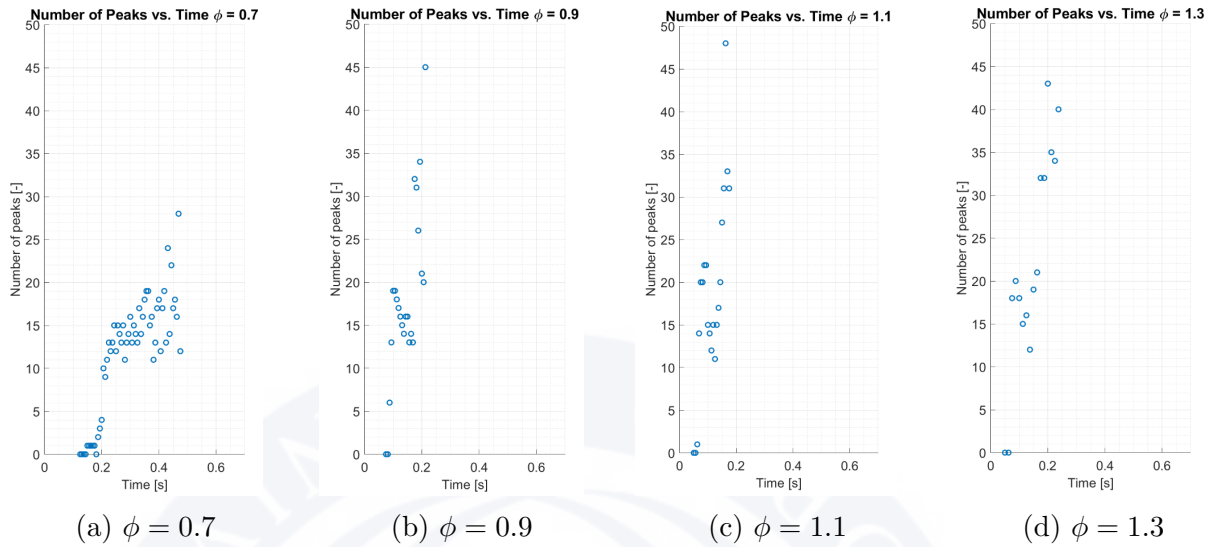


Figure 3.2: Peaks Evolution with Time

Finally, if the evolution of each experiment is analyzed, it can be appreciated how the instabilization time (time to appear the first instabilities) is also affected by the equivalence ratio, being decreased as the mixture becomes richer and is quite similar for all the configurations with $\phi > 1$, which sounds logical as the time of reaction of a mixture is shorter as closer to the stoichiometric reaction. On the other hand the time for the flame to reach lateral and frontal sides of the rectangle follows the same behaviour, being shorter as they are closer to the stoichiometric mixture; as well as in the previous case, the velocity of reaction is proportional to the concentration of propane and to the stoichiometry of the reaction.

3.2 Lengths

The length of the flame is the less varying result for the equivalence ratios configurations. Although it can be seen that exists an exponential growth of the whole length of the flame with time for all the configurations with some exceptions, in which the total length decreases in the last stages of the evolution due to the exit of the boundaries Fig. 3.3 (a); the total length adapts quite good to the perimeter of the cell being for all cases around 2 meters in its last frame.

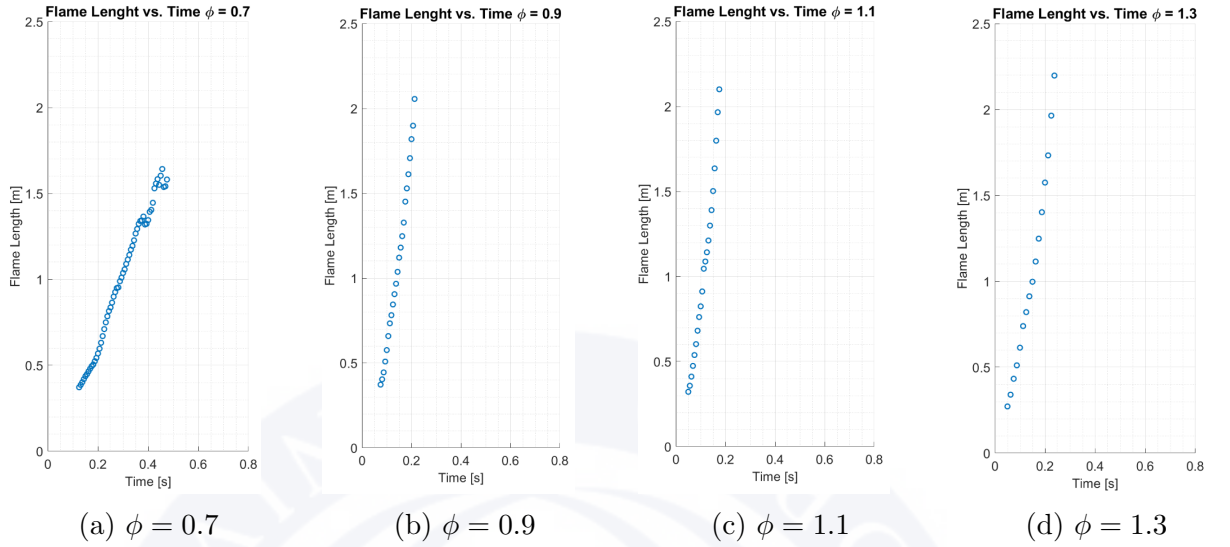


Figure 3.3: Length Evolution with Time

The small variations for the different ϕ mixtures, are due to the instabilities generated in the front: with more instabilities, the length becomes bigger due to the appearance of lobes in the interphase. So as commented in the last subsection 3.1, it is appreciable an increasing tendency with ϕ .

On the other hand, studying the lobe length results, it can be come up the same conclusion reached in the analysis of the evolution of instabilities. At the beginning of the combustion small disturbances appear, which start growing with time; then some of the lobes disappear and merge creating bigger cells to finally emerge some tiny instabilities at the beginning and end of the contour, and for the most unstable combustions, at the central lobes Fig. 3.4 (c & d).

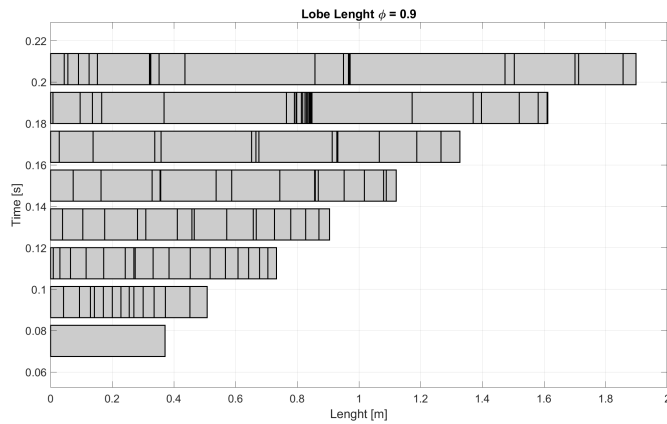
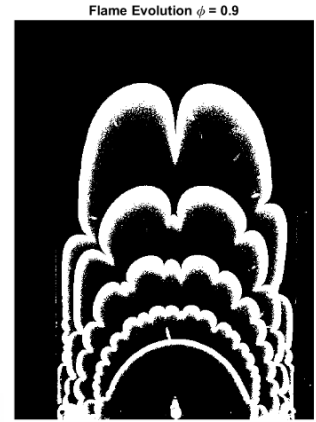
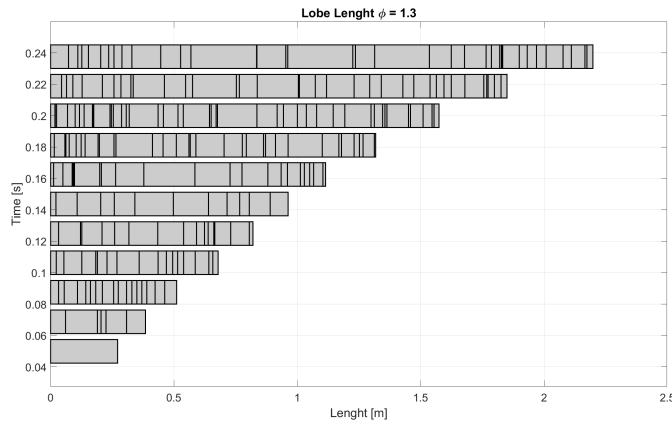
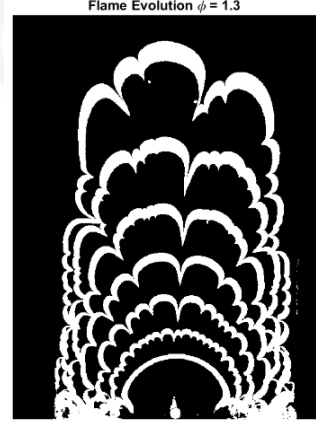
(a) Lobes $\phi = 0.9$ (b) Evolution $\phi = 0.9$ (c) Lobes $\phi = 1.3$ (d) Evolution $\phi = 1.3$

Figure 3.4: Lobe Lengths

It's also remarkable how the difference of equivalence ratios affects the lobe length distribution. In all the cases it can be appreciated how a homogeneous cellular length is adopted at the first stages of the combustion, meanwhile once the flow develops, the rich mixtures create more lobes of similar lengths and the lean ones have huge differences between its main and secondary cells.

3.3 Motion

As one of the most complex parts of the project, the local velocities of the flame front, show up the most interesting results.

At the beginning of the process, the flame expands radially from the igniter at the center left side. In this stage it can be observed how some small variations appear on the vector field due to stretching in the peaks of the lobes and some turning at the

front and rear edges of the flame. These effects will be increased with the evolution of the flame.

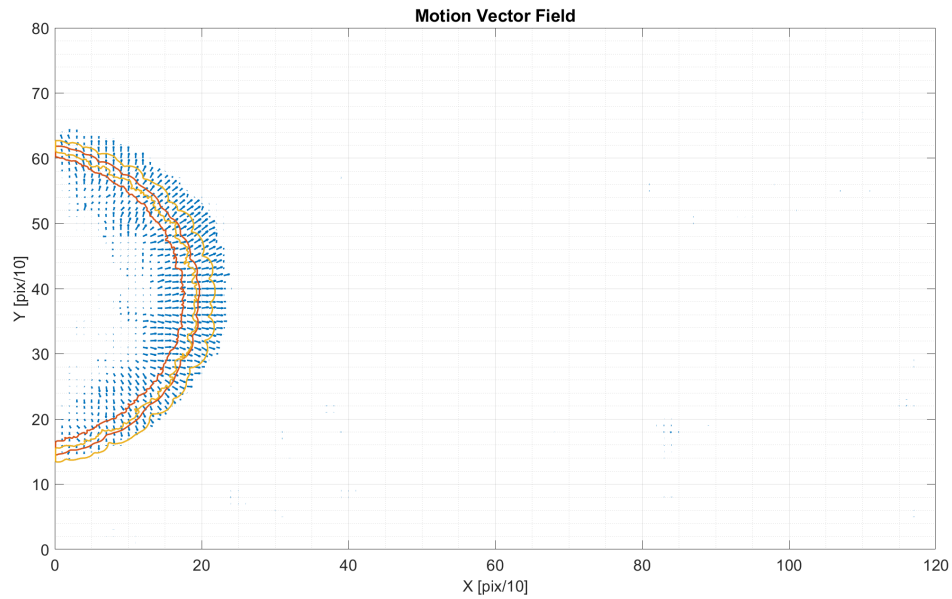


Figure 3.5: Radial Expansion

At some time, the flow field adapts a new pattern. As the algorithm is able to not only compute the motion for the contour but for the surrounding burnt and unburned gases, it can be appreciated how the flow of the unburned gases at the frontal part of the flame start to reverse going in the opposite direction to the combustion [3]. This recirculation is practically symmetrical and its motivated by bounding surfaces of the cell, that is why it affects only the central part of the flow. These results accord with the potential flow of fluid mechanics.

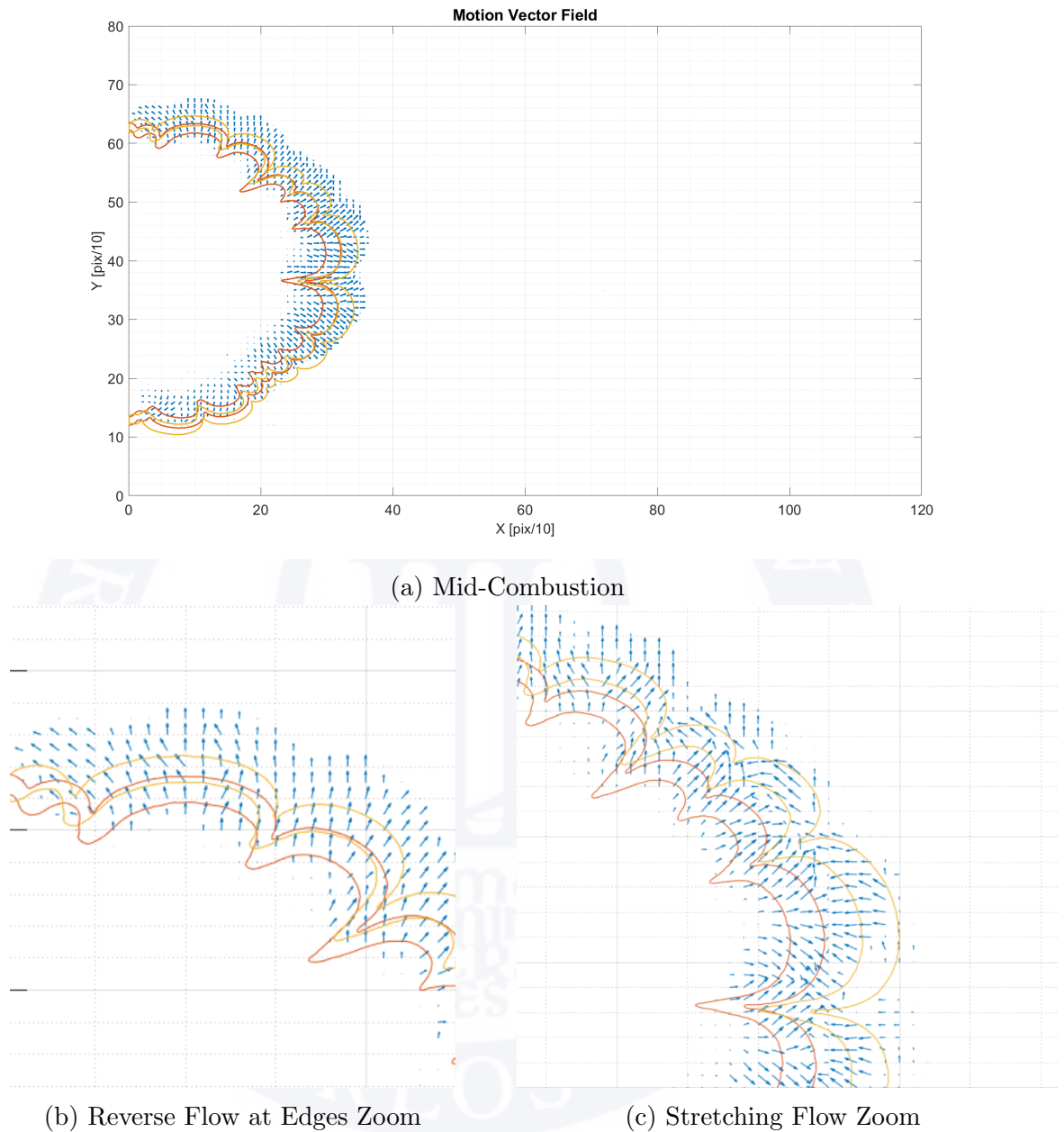
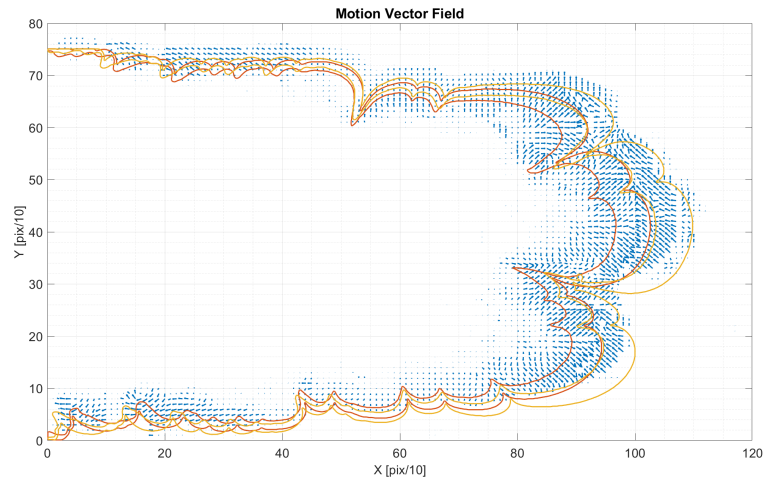


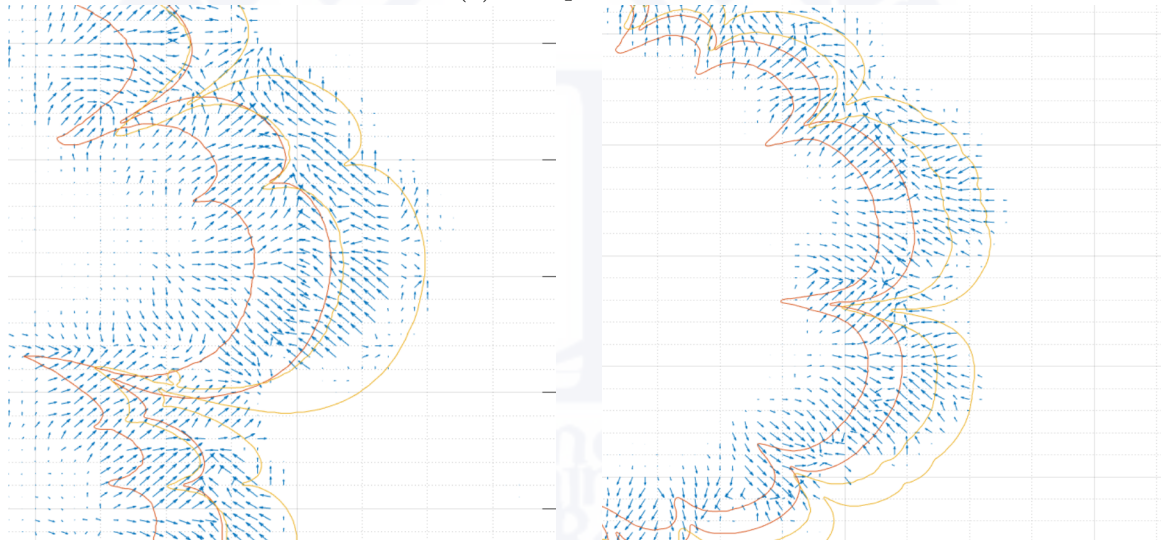
Figure 3.6: Mid-Combustion Flow Facts

At this point, the results display how the burnt gases merge into the peaks by the stretching of the front and how the flow in the flame's edges is completely turned.

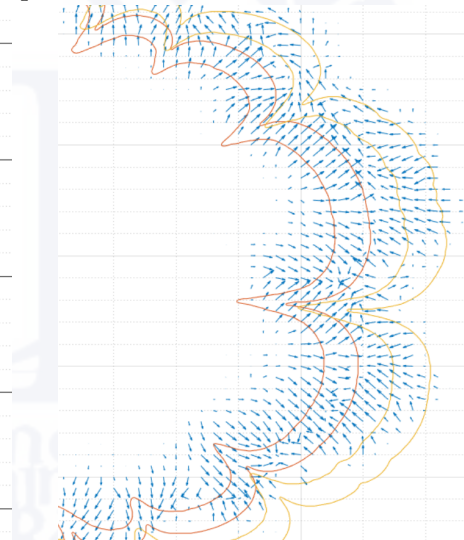
Finally, the last stages of the combustion exhibit an enhancement of the effects previously commented and it can be distinguished an interphase on the flow field situated in the central part of the flame exactly after the front, between the burnt and unburned flows (red and yellow graphs respectively).



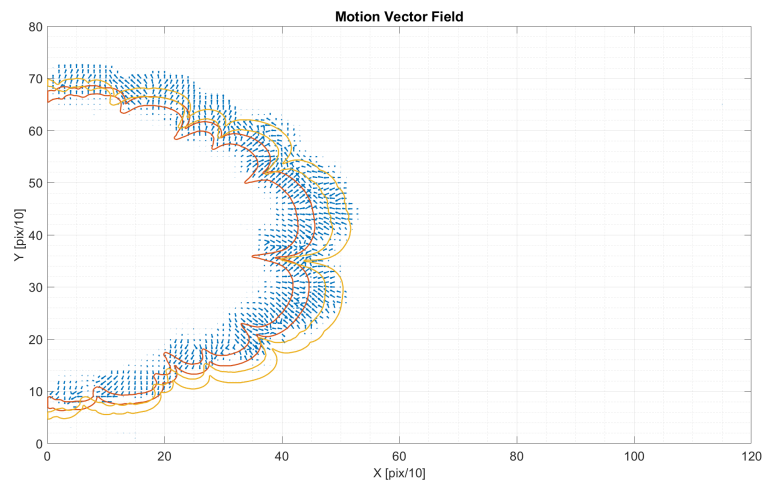
(a) Interphase Flow



(b) Interphase Flow Zoom



(c) Recirculation Flow Zoom

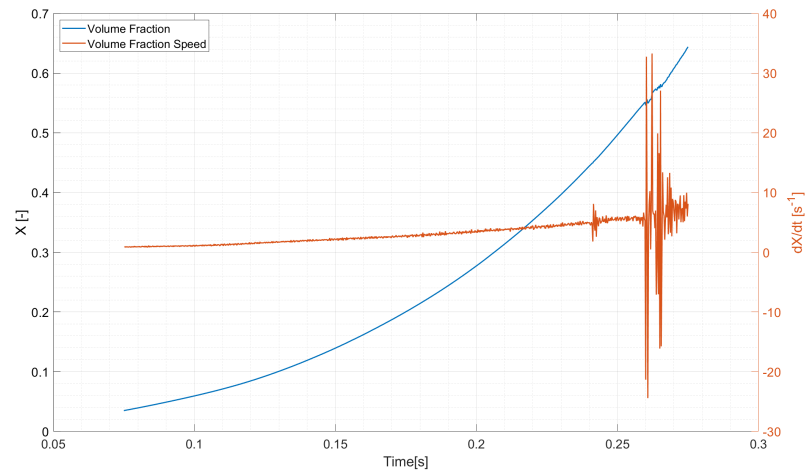


(d) Recirculation

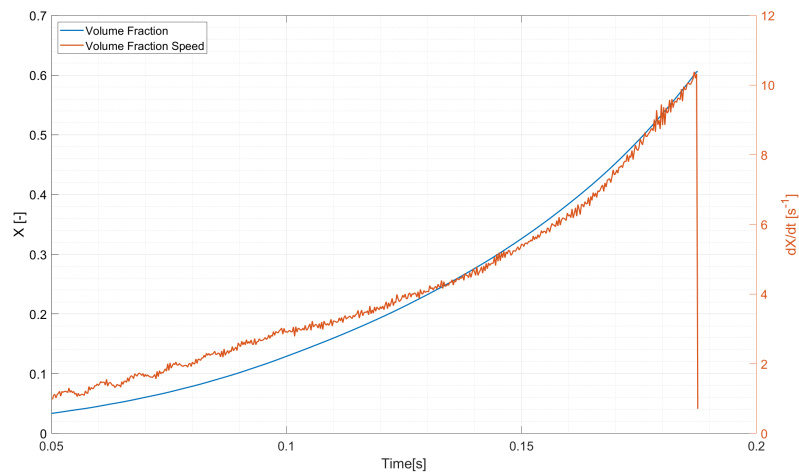
Figure 3.7: Late-Combustion Flow Facts

3.4 Burnt Velocity

Lastly, if the burnt velocity results are carefully analysed, several particularities can be observed. The first and most obvious one is the parabolic increase of the volume with time for all the experiments. This behaviour agrees with the length results showed before as the evolution of the perimeter is virtually the same for area and length, excluding the low amplitude vibrations produced in the volume due to the instabilities propagation. Moreover, the ϕ influence on X exhibits a greater volume burnt as approaching to 1.



(a) Linear Increase $\phi = 0.8$



(b) Non-Linear Increase $\phi = 1.2$

Figure 3.8: Burning Behaviours

In the velocity case, the results display an amplitude variable signal which can be observed as being noisy for most of the cases. Here it can be observed two different behaviours: the first one is exhibited by the lean configurations, a low linear increase of the mean amplitude with time; however, for rich mixtures, the mean amplitude increases non linearly with time while they tend to be less noisy than the lean mixtures. Sudden and large increments on this function are mostly due to errors in raw images and decrease of the flame's length due to exiting the cell.



Chapter 4

Conclusion

The main goal of this project was to study the evolution of a flame and its consequences through a 2D experiment, the Hele-Shaw Cell, in order to study the dynamics of the fluid. Once done, it would be possible to estimate its behaviour, improving the main characteristics of combustion and engines. This experiment and its analysis was based on the instabilities emerged during the propagation in the front of the flame. By studying them and relating the results with fluid dynamics theory.

Once the experiment was finalized, the subsequent analysis were performed. This data obtained was processed based on the image processing, change to curvilinear reference frame and the application of Block Matching to create a flow field. While all this data was fitted to easily reading information, some parameters were described to characterize the instabilities and so flame evolution. This new application of the algorithm is the main and revolutionary part of the study as it allows to estimate the stream lines of the flame and localize the influences of the experiment's environment into the stability of the contour as well as the local velocities, displacements and behaviour of any specific point of analysis, specifically in this study the peaks of the signal.

By applying this method to several equivalence ratios of the mixture propane-air a global view of the stoichiometry's influence on the parameters previously defined could be observed. Those results reinforce the instabilities theory while show that a system is more stable and faster as it is closer to its stoichiometric values, producing a smooth propagation that would lead to better efficiencies of combustion, emission and noises.

Finally, despite the main goals of study in this project were achieved with the implementation of new techniques, further analysis could be done to this experiment using image and signal processing in order to fully determine the flame's instabilities with more complex theories [11]

Bibliography

- [1] C. S. 2. Development plan. Technical report, Clean Sky, 2017.
- [2] C. Almarcha, J. Quinard, B. Denet, E. Al-Sarraf, J. Laugier, and E. Villiermaux. Experimental two dimensional cellular flames. *Physics of Fluids*, 27(9):091110, 2015.
- [3] T. F. Balsa. Secondary flow in a hele-shaw cell. *Journal of Fluid Mechanics*, 372:25–44, 1998.
- [4] B. D. Bellows, M. K. Bobba, J. M. Seitzman, and T. Lieuwen. Nonlinear flame transfer function characteristics in a swirl-stabilized combustor. *Journal of Engineering for Gas Turbines and Power*, 129(4):954–961, 2007.
- [5] F. Boudy. Nonlinear dynamics and control analysis of combustion instabilities based on the “flame describing function” (fdf). 2012.
- [6] R. Brown. fitellipse.m :fit ellipses to 2d points using linear or nonlinear least squares, 2016.
- [7] V. V. Bychkov. Nonlinear equation for a curved stationary flame and the flame velocity. *Physics of fluids*, 10(8):2091–2098, 1998.
- [8] D. Calvo. Experimental investigation of non linear flame dynamics. Master’s thesis, UNIVERSIDAD CARLOS III DE MADRID, 2016.
- [9] M. Chan, Y. Yu, and A. Constantinides. Variable size block matching motion compensation with applications to video coding. *IEE Proceedings I (Communications, Speech and Vision)*, 137(4):205–212, 1990.
- [10] S. H. Chan, D. T. Vĩ, and T. Q. Nguyen. Subpixel motion estimation without interpolation. Technical report, 2010.
- [11] C. Clanet and G. Searby. First experimental study of the darrieus-landau instability. *Physical Review Letters*, 80(17):3867, 1998.
- [12] C. Clanet, G. Searby, and P. Clavin. Primary acoustic instability of flames propagating in tubes: cases of spray and premixed gas combustion. *Journal of Fluid Mechanics*, 385:157–197, 1999.
- [13] E. COMMISSION. Communication from the commission to the european parliament, the council, the european economic and social committee and the committee of the regions. Technical report, EUROPEAN COMMISSION, 2016.

- [14] L. Crocco and S.-I. Cheng. Theory of combustion instability in liquid propellant rocket motors. 1956.
- [15] K. Dabov, A. Foi, V. Katkovnik, and K. Egiazarian. Image denoising with block-matching and 3d filtering. In *Image Processing: Algorithms and Systems, Neural Networks, and Machine Learning*, volume 6064, page 606414. International Society for Optics and Photonics, 2006.
- [16] G. Darrieus. Propagation d'un front de flamme. *La Technique Moderne*, 30:18, 1938.
- [17] Y. Dazhi, W. M. Walsh, D. Zibo, P. Jirutitijaroen, and T. G. Reindl. Block matching algorithms: Their applications and limitations in solar irradiance forecasting. *Energy Procedia*, 33:335–342, 2013.
- [18] D. Fernández-Galisteo, V. N. Kurdyumov, and P. D. Ronney. Analysis of premixed flame propagation between two closely-spaced parallel plates. *Combustion and Flame*, 190:133–145, 2018.
- [19] J. A. García, J. Fdez-Valdivia, F. J. Cortijo, and R. Molina. A dynamic approach for clustering data. *Signal Processing*, 44(2):181–196, 1995.
- [20] S. Golemati, A. Sassano, M. J. Lever, A. A. Bharath, S. Dhanjil, and A. N. Nicolaides. Carotid artery wall motion estimated from b-mode ultrasound using region tracking and block matching. *Ultrasound in Medicine and Biology*, 29(3):387–399, 2003.
- [21] A. K. Idris. A numerical study on premixed laminar flame front. instabilities in thermoacoustic systems. Master's thesis, Universität München, 2016.
- [22] J. Jain and A. Jain. Displacement measurement and its application in inter-frame image coding. *IEEE Transactions on communications*, 29(12):1799–1808, 1981.
- [23] S. Kang, S. Baek, and H. Im. Effects of heat and momentum losses on the stability of premixed flames in a narrow channel. *Combustion Theory and Modelling*, 10(4):659–681, 2006.
- [24] H. Krediet, C. Beck, W. Krebs, S. Schimek, C. Paschereit, and J. Kok. Identification of the flame describing function of a premixed swirl flame from les. *Combustion Science and Technology*, 184(7-8):888–900, 2012.
- [25] L. Landau. On the theory of slow combustion. *Acta Phys.*, 19:77–85, 1944.
- [26] B. Mugridge. Combustion driven oscillations. *Journal of Sound and Vibration*, 70(3):437–452, 1980.
- [27] T. Nakai, T. Okakura, and K. Arakawa. Face recognition across age progression using block matching method. In *Communications and Information Technologies (ISCIT), 2010 International Symposium on*, pages 620–625. IEEE, 2010.

- [28] S. Ourselin, A. Roche, S. Prima, and N. Ayache. Block matching: A general framework to improve robustness of rigid registration of medical images. In *International Conference on Medical Image Computing And Computer-Assisted Intervention*, pages 557–566. Springer, 2000.
- [29] P. Pelcé. *Dynamics of Curved Fronts (Perspectives in Physics)*(Boston, MA: Academic). 1988.
- [30] A. Puri, H.-M. Hang, and D. Schilling. An efficient block-matching algorithm for motion-compensated coding. In *Acoustics, Speech, and Signal Processing, IEEE International Conference on ICASSP'87.*, volume 12, pages 1063–1066. IEEE, 1987.
- [31] L. Rayleigh. *The explanation of certain acoustical phenomena*, volume 8, pages 536–542. 1878.
- [32] D. Reguera, L. L. Bonilla, and J.-M. Rubi. *Coherent Structures in Complex Systems: Selected Papers of the XVII Sitges Conference on Statistical Mechanics Held at Sitges, Barcelona, Spain, 5–9 June 2000. Preliminary Version*, volume 567. Springer Science & Business Media, 2001.
- [33] S. S. Sadeghi, S. Tabejamaat, M. Baigmohammadi, and J. Zarvandi. An experimental study of the effects of equivalence ratio, mixture velocity and nitrogen dilution on methane/oxygen pre-mixed flame dynamics in a meso-scale reactor. *Energy conversion and management*, 81:169–183, 2014.
- [34] P. G. Saffman and F. S. G. TAYLOR. The penetration of a fluid into a porous medium or hele-shaw cell containing a more viscous liquid. pages 155–174, 1988.
- [35] B. Vermeulen. Cartesian to curvilinear coordinate forward and backward transformation, 2016.
- [36] E. Viarani. Extraction of traffic information from images at deis. In *Image Analysis and Processing, 1999. Proceedings. International Conference on*, pages 1073–1076. IEEE, 1999.
- [37] S. Villena, M. Vega, S. D. Babacan, R. Molina, and A. K. Katsaggelos. Bayesian combination of sparse and non-sparse priors in image super resolution. *Digital Signal Processing*, 23(2):530–541, 2013.
- [38] N. Yoder. peakfinder.m : Quickly finds local maxima (peaks) or minima (valleys) in a noisy signal., 2009.